Mathematical models and numerical analysis of the conduction and valence band engineering in cylindrical quantum dots

Prabhakar, S., Takhtamirov, E. and Melnik, R.

Applied Mathematics and Informatics (European Conference for the Applied Mathematics and Informatics, Greece, Dec, 2010), Eds. N. Mastorakis et al, pp. 201-206, 2010,

ISSN: 1792-7390 || ISBN: 978-960-474-260-8.

Editors: Nikos Mastorakis, Valeri Mladenov,
Metin Demiralp, Zoran Bojkovic

Applied Mathematics & Informatics

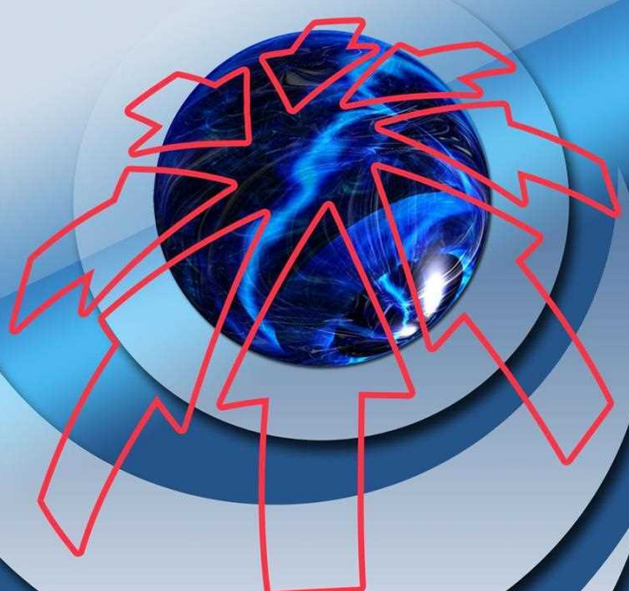

Applied Mathematics & Informatics

European Conference for the Applied Mathematics and Informatics

Vouliagmeni, Athens, Greece, December 29-31, 2010

ISBN: 978-960-474-260-8
PRINT VERSION ISSN: 1792-7390
ELECTRONIC VERSION ISSN: 1792-7404

APPLIED MATHEMATICS and INFORMATICS

European Conference for the APPLIED MATHEMATICS and INFORMATICS

Vouliagmeni, Athens, Greece
December 29-31, 2010

ISSN: 1792-7390
ISBN: 978-960-474-260-8

APPLIED MATHEMATICS and INFORMATICS

European Conference for the APPLIED MATHEMATICS and INFORMATICS

Vouliagmeni, Athens, Greece
December 29-31, 2010

All papers of the present volume were peer reviewed by two independent reviewers. Acceptance was granted when both reviewers' recommendations were positive.
See also: http://www.worldses.org/review/index.html

ISSN: 1792-7390
ISBN: 978-960-474-260-8

European Society for Applied Mathematics - EuroSAM

Mathematical models and numerical analysis of the conduction and valence band eigenenergy in cylindrical quantum dots

SANJAY PRABHAKAR, EDUARD TAKHTAMIROV and RODERICK MELNIK
Department of Mathematics
Wilfrid Laurier University
75 University Ave W, Waterloo, ON N2L 3C5
CANADA
rmelnik@wlu.ca; htpp://www.m2netlab.wlu.ca

Abstract:- We develop a mathematical model for the analysis of conduction and valence band eigenenergy in quantum dots. We apply this model to study the band structure of low dimensional semiconductor nanostructures (LDSNs) such as wurtzite AlN/GaN quantum dots in cylindrical coordinates in the presence of applied magnetic field along z-direction. We use a finite element method to solve the resulting model and to obtain eigenvalues and wave functions of cylindrical quantum dots. We provide details of the methodology of solution and appropriate boundary conditions. A special attention is given to the case of applied magnetic field along z-direction where we found localized eigenstates and wave functions in the conduction and valence bands for which our results open new possibilities for the design of such optoelectronics devices where the combination of electron-hole pairs can be used as tuning parameters.

Key-Words:- Quantum dots, Mathematical models, Spintronics, Wurtzite structures, Localized states, Finite Element Method.

1 Introduction

Nanostructures based on wide band gap semiconductor materials such as AlN/GaN quantum dots have attracted significant attention due to their current and potential applications in optical, optoelectronic and electronic devices, as well as in bionanotechnology. The small, arbitrary shaped crystal structures can be realized to obtain quantum size effects by patterning techniques with the help of electron beam lithography, optical lithography, x-ray lithography and others. Self-assembled QDs are grown by Stranski-Krastanov process are of special interest because of their potential applications in QDs lasers, light emitting diodes as qubits for quantum computation, and other applications [1,2,3,4].

A subject that has not been studied in detail in the context of AlN/GaN quantum dots, however, is related to localized eigenstates in valence bands of wurtzite structures of cylindrical shape. This is the subject of the present investigation. Our approach is closely related to that of [5] but differs in a way that we include the external magnetic field along z-direction and derive the equations for holes in the valence band in cylindrical coordinates

ISBN: 978-960-474-260-8

with a different procedure.

In this paper, we also present a numerical analysis of the band structure of single AlN/GaN QDs under the influence of applied magnetic field along z-direction. By using the Finite Element Method (FEM), we study the eigenvalues and wave functions of the electrons in the conduction and valence bands.

2 Mathematical Model

In this section, we develop a theoretical model of the Hamiltonian, focusing on both the conduction and valence bands of quantum wurtzite system in cylindrical coordinates. The detailed theoretical model for the conduction band of wurtzite structures in cylindrical coordinates was explained in [4]. The results on the valence band Hamiltonian in cylindrical coordinates will be published elsewhere [6].

2.1 Conduction band Hamiltonian in cylindrical coordinates

We consider the motion of the electron confined along the z-direction in the presence of magnetic field oriented along a direction perpendicular to the plane of two dimensional electron gas (2DEG). Therefore, the total Hamiltonian of an electron including Rashba spin orbit interaction in cylindrical coordinates can be written as [4]

$$H = \begin{bmatrix} h_+ & \alpha_R \left[\frac{\partial}{\partial r} + \frac{1}{r}\left(j+\frac{1}{2}\right) + \frac{eBr}{2\hbar}\right] \\ \alpha_R \left[-\frac{\partial}{\partial r} + \frac{1}{r}\left(j-\frac{1}{2}\right) + \frac{eBr}{2\hbar}\right] & h_- \end{bmatrix}, \tag{1}$$

where

$$\begin{aligned} h_\pm &= -\frac{\hbar^2}{2m_0}\left[\frac{1}{r}\frac{\partial}{\partial r}\frac{r}{m_e^\perp}\frac{\partial}{\partial r} + \frac{\partial}{\partial z}\frac{1}{m_e^\parallel}\frac{\partial}{\partial z} - \frac{1}{r^2}\frac{1}{m_e^\perp}\left(j \mp \frac{1}{2}\right)^2\right] \\ &\quad + \frac{1}{8}m_e^\perp\omega_c^2\rho^2 + \frac{\hbar\omega_c}{2}\left(j \mp \frac{1}{2}\right) \mp \frac{1}{2}g_0\mu_B B + E_c, \end{aligned} \tag{2}$$

$\omega_c = \frac{eB}{m_e^\perp c}$ is the cyclotron frequency, $m_e^\perp$ and $m_e^\parallel$ are the effective masses, c is the velocity of light and B is the magnetic field along z-direction. Also, α_R is the Rashba coefficients. Here we consider the experimentally reported bulk material parameters $g_0 = 1.9885$ for AlN and $g_0 = 1.9510$ for GaN material from Ref. [7]

2.2 Valence band Hamiltonian in Cartesian coordinates

We start from the steady state Schrödinger equation in the effective-mass approximation [9],

$$HF = \left(H^0 + H^{so} + H^k + H^\varepsilon\right)F = EF. \tag{3}$$

Equation (3) was constructed by using the orthogonal and normalized Bloch zone-center functions for the potential well material, which are written as $\mathbf{u} = (u_x, u_y, u_z)$. The functions $u_x = u_x(\mathbf{r})$ and $u_y = u_y(\mathbf{r})$ transform as the Cartesian coordinates x and y belonging to the representation Γ_6 of the space group C_{6v}, and $u_z = u_z(\mathbf{r})$ transform as the coordinate z along c-axis of the wurtzite structure in Γ_1 notation [8]. The envelop

ISBN: 978-960-474-260-8

function $F = F(\mathbf{r})$ has three components: $F = (F_x, F_y, F_z)^T$, where T stands for the transpose of a vector, so that total wave function $\Psi = \Psi(\mathbf{r})$ can be written as,

$$\Psi = \sum_{j=x,y,z} u_j F_j = \mathbf{uF}. \tag{4}$$

The basis functions $\mathbf{u}$ are spinless, so each envelope function element F_j act as a spinor. The Hamiltonian parts H^0, H^{so} and H^k in Eq. 3 can be written as [8],

$$H^0 = \begin{pmatrix} U_6 & 0 & 0 \\ 0 & U_6 & 0 \\ 0 & 0 & U_1 \end{pmatrix}, \tag{5}$$

$$H^{so} = i \begin{pmatrix} 0 & -\Delta_2\sigma_z & \Delta_3\sigma_y \\ \Delta_2\sigma_z & 0 & -\Delta_3\sigma_x \\ -\Delta_3\sigma_y & \Delta_3\sigma_x & 0 \end{pmatrix}, \tag{6}$$

$$H^k = \begin{pmatrix} L_1k_x^2 + M_1k_y^2 + M_2k_z^2 & N_1k_xk_y & N_2k_xk_z \\ N_1k_xk_y & M_1k_x^2 + L_1k_y^2 + M_2k_z^2 & N_2k_yk_z \\ N_2k_xk_z & N_2k_yk_z & M_3\left(k_x^2 + k_y^2\right) + L_2k_z^2 \end{pmatrix}, \tag{7}$$

where $U_6 = U(\mathbf{r})$ and $U_1 = U_1(\mathbf{r})$ are the edges of the bands Γ_6 and Γ_1, respectively, which may contain an external scalar potential. σ_i are the Pauli matrices. L_1, L_2, M_1, M_2, N_1 and N_2 are the material parameters for the potential well semiconductor, and $\hbar k$ is the momentum operator. In Eq. (7), we choose the relation $L_1 - M_1 = N_1$.

2.2.1 Valence band Hamiltonian in cylindrical coordinates

All Cartesian elements from Eq. 3 can be changed into cylindrical coordinates (r,ϕ,z) by letting $x = r\cos\phi$ and $y = r\sin\phi$. Here we suppose the envelope functions $\bar{\bar{F}} = e^{im\phi}f(r,z)/\sqrt{2\pi}$. The eigenvalues m of the operator of the z-component of the total angular momentum should be half-integer: $m = \pm 1/2, \pm 3/2, ...$ The detailed procedure for the conversion of the Hamiltonian in cylindrical coordinates will be published elsewhere [6]. Here we present the main result. The Hamiltonian in cylindrical coordinates can be written as

$$\bar{\bar{H}}^k = -\begin{pmatrix} h_{11} & iL_1\nabla_r\frac{\mathbf{m}}{r} - iM_1\left[\frac{\mathbf{m}}{r}\nabla_r + \frac{\mathbf{m}}{r^2}\right] & N_2\nabla_r\nabla_z \\ iL_1\left[\frac{\mathbf{m}}{r}\nabla_r + \frac{\mathbf{m}}{r^2}\right] - iM_1\nabla_r\frac{\mathbf{m}}{r} & h_{22} & iN_2\frac{\mathbf{m}}{r}\nabla_z \\ N_2\left[\nabla_r + \frac{1}{r}\right]\nabla_z & iN_2\frac{\mathbf{m}}{r}\nabla_z & h_{33} \end{pmatrix}, \tag{8}$$

where

$$h_{11} = L_1\left[\nabla_r^2 + \nabla_r\frac{1}{r}\right] - M_1\frac{\mathbf{m}^2}{r^2} + M_2\nabla_z^2, \tag{9}$$

$$h_{22} = M_1\left[\nabla_r^2 + \nabla_r\frac{1}{r}\right] - L_1\frac{\mathbf{m}^2}{r^2} + M_2\nabla_z^2, \tag{10}$$

$$h_{33} = M_3\left[\nabla_r^2 + \frac{1}{r}\nabla_r - \frac{\mathbf{m}^2}{r^2}\right] + L_2\nabla_z^2, \tag{11}$$

and the matrix $\mathbf{m}$ has the simple form

$$\mathbf{m} = \begin{pmatrix} m - \frac{1}{2} & 0 \\ 0 & m + \frac{1}{2} \end{pmatrix}. \tag{12}$$

ISBN: 978-960-474-260-8

The spin-orbit interaction Hamiltonian (6) transforms into the Hamiltonian $\tilde{H}^{so} = SH^{so}S^{-1}$:

$$\tilde{H}^{so} = i \begin{pmatrix} 0 & -\triangle_2\sigma_z & \triangle_3\sigma_\phi \\ -\triangle_2\sigma_z & 0 & -\triangle_3\sigma_r \\ -\triangle_2\sigma_\phi & \triangle_2\sigma_r & 0 \end{pmatrix}, \tag{13}$$

where $\sigma_r = \sigma_x \exp(i\phi\sigma_z)$ and $\sigma_\phi = \sigma_y \exp(i\phi\sigma_z)$.

The Hamiltonian (13) depends on ϕ and does not commute with the operator $-i\nabla_\phi$. To eliminate this dependence, we note first that

$$e^{i\frac{\phi}{2}\sigma_z}\sigma_r e^{-i\frac{\phi}{2}\sigma_z} = \sigma_x, \qquad e^{i\frac{\phi}{2}\sigma_z}\sigma_\phi e^{-i\frac{\phi}{2}\sigma_z} = \sigma_x, \tag{14}$$

and then we construct a unitary transformation: $\tilde{S}\tilde{F} = \tilde{\tilde{F}}$, where

$$\tilde{S} = \begin{pmatrix} e^{i\frac{\phi}{2}\sigma_z} & 0 & 0 \\ 0 & e^{i\frac{\phi}{2}\sigma_z} & 0 \\ 0 & 0 & e^{i\frac{\phi}{2}\sigma_z} \end{pmatrix}. \tag{15}$$

2.2.2 Inclusion of external magnetic field

Consider an external magnetic field B_z applied along the z-axis, which does not break the cylindrical symmetry of the system. We use the symmetric gauge for the vector potential $A = (A_x, A_y, A_z) = (-yB/2, -xB/2, 0)$ in cylindrical coordinates, or $A = (A_r, A_\phi, A_z) = (0, rB_z/2, 0)$ in cylindrical coordinates. The kinetic momentum operator is $K = k + eA/(\hbar c)$, where e is the electronic charge. Also, we have to include the effective Pauli term in the Hamiltonian (3) as,

$$H^B = \begin{pmatrix} \frac{1}{2}g_0\mu_B B\sigma_z & -\frac{ie}{2\hbar c}QB & 0 \\ 0 & \frac{1}{2}g_0\mu_B B\sigma_z & 0 \\ \frac{ie}{2\hbar c}QB & 0 & \frac{1}{2}g_0\mu_B B\sigma_z \end{pmatrix}, \tag{16}$$

where $g_0 = 2$ is the free electron g-factor, μ_B is the Bohr magneton, and Q is a material specific parameter [10]. In a way similar to that discussed in the previous section, in the presence of external magnetic field along z-direction, one can write the Hamiltonian in cylindrical coordinates as

$$\bar{\bar{H}}^k = -\begin{pmatrix} h_{11} & h_{12} & N_2\nabla_r\nabla_z \\ h_{12} & h_{22} & iN_2\frac{\mathbf{m}}{r}\nabla_z \\ N_2\left[\nabla_r + \frac{1}{r}\right]\nabla_z & iN_2\frac{\mathbf{m}}{r}\nabla_z & h_{33} \end{pmatrix}, \tag{17}$$

where h_{11}, h_{22} and h_{33} given by (9) - (11) and

$$h_{12} = iL_1\{\mathbf{m}, \nabla_r\}_+ \frac{1}{2r} - iM_1\left[\frac{1}{2r}\{\mathbf{m}, \nabla_r\} + \frac{\mathbf{m}}{r^2}\right], \tag{18}$$

$$h_{21} = iL_1\left[\frac{1}{2r}\{\mathbf{m}, \nabla_r\}_+ + \frac{\mathbf{m}}{r^2}\right] - iM_1\{\mathbf{m}, \nabla_r\}_+ \frac{1}{2r}, \tag{19}$$

and the matrix $\mathbf{m}$ has the simple form

$$\mathbf{m} = \begin{pmatrix} \frac{e}{2\hbar c}B_z r^2 + m - \frac{1}{2} & 0 \\ 0 & \frac{e}{2\hbar c}B_z r^2 + m + \frac{1}{2} \end{pmatrix}. \tag{20}$$

ISBN: 978-960-474-260-8

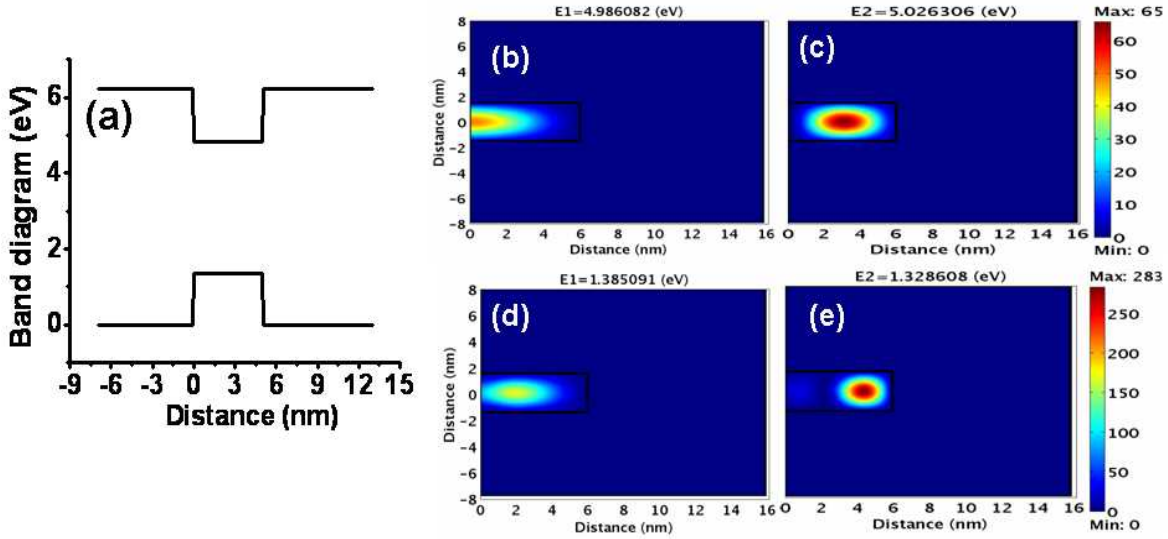

Figure 1: (a) Flat conduction and valence band diagram of AlN/GaN quantum dot along z-direction; (b) Ground state eigenvalues and wave fucntions of electron in the flat conduction band; (c) First excited state eigenvalues and wave fucntions of electron in the flat conduction band; (d) Ground state eigenvalues and wave functions of holes in the flat valence band. (e) First excited state eigenvalues and wave fucntions of holes in the flat valence band.

3 Results and Discussions

We consider GaN as a quantum dot material embedded into the host material of AlN. We apply Dirichlet boundary conditions far away from the quantum dot. In other words, it is assumed that the electron wave function is zero sufficiently far away from the quantum dot. Further, we consider the electron wave function to be continuous at the center and at the interface between AlN/GaN quantum dot. As a result, we apply Neumann boundary condition at the center and at the interface of the AlN/GaN quantum dot. We have found the localized eigenstates and eigenvalues in the conduction and valence bands of wurtzite AlN/GaN quantum dots. The electron and hole eigenstates found in the conduction and valence bands recombine each other in the form of electron-hole pairs and produce photons. These photons have a wide range of applications in light emitting diodes, semiconductor lasers and other areas.

In Fig. 1, we plotted the conduction and valence band diagram of a AlN/GaN quantum dot along z-direction by choosing the appropriate band discontinuity and band offset at the interface of the AlN/GaN heterojunction. We adopted the Finite Element Method to solve the coupled problem associated with Hamiltonian (1) for an electron in cylindrical coordinates in the flat conduction band. The eigenvalues and the wave functions of the ground and first excited states of the electron are shown in Fig. 1(a) and (b). Here we have estimated the ground and first excited states eigenvalues in the conduction band as 4.986082 eV and 5.026306 eV, respectively. The ground and first excited states of the electron in the valence band have been found by solving the corresponding eigenvalue problem for the Hamiltonian (17). The ground and first excited states of the electron wave functions are shown in Fig. 1(d) and (e). Here, we have estimated the ground and first excited states

ISBN: 978-960-474-260-8

eigenvalues of the electron as 1.385091 eV and 1.328608 eV. The electron found in the localized eigenstates at 4.986082 eV in the conduction band has an opportunity to recombine with the hole found in the localized eigenstates at 1.385091 eV in the valence band. The recombination of electron-hole pairs generates photons which is the fundamental to the operation of many optoelectronic semiconductor devices, such as photodiodes, Light Emitting Diodes (LEDs) and laser diodes among others.

4 Conclusions

In this paper, we have developed a mathematical model for the valence band of a quantum dot in cylindrical coordinates with wurtzite symmetry in the presence of external magnetic field along z-direction. We solved the coupled Schrödinger equation in the conduction and valence bands separately and found the localized eigenstates and wave functions. The localized eigenstates for electrons and holes in their corresponding bands will recombine to form electon-hole pairs. The photons generated by electron-hole pairs during the recombination process has a wide range of applications for novel optoelectronic devices.

Acknowledgments:- This work was supported by the NSERC and the CRC program, Canada.

References:

1. L. C. Lew Yan Voon, C. Galeriu, B. Lassen, M. Willatzen, and R. Melnik, Electronic structure of wurtzite quantum dots with cylindrical symmetry, Appl. Phys. Lett. 87, 041906 (2005).
2. B. Daudin, F. Widmann, G. Feuillet, Y. Samson, and J. L. Rouvière, Stranski-Krastanov growth mode during the molecular beam epitaxy of highly strained GaN, Phys. Rev. B 56, R7069 (1997); P. Micheler, Single quantum dots, Fundamentals, Applications and New Concepts, ISBN 3-540-14022-02, Springer 2003.
3. S. R. Patil and R. Melnik, Thermoelectromechanical effects in quantum dots, Nanotechnology 20, 125402 (2009).
4. S. Prabhakar and R. Melnik, Influence of electromechanical effects and wetting layers on band structures of AlN/GaN quantum dots and spin control, J. Appl. Phys., 108, 064330 (2010).
5. L. Voon, C. Galeriu, B. Lassen, M. Willatzen, and R. Melnik, Electronic structure of wurtzite quantum dots with cylindrical symmetry, Appl. Phys. Lett. 87, 041906 (2005).
6. S. Prabhakar, E. Takhtamirov and R. Melnik, Valence band Hamiltonian for wurtzite structure in cylindrical coordinates and spin control, J. Appl. Phys., in preparation.
7. M. W. Bayerl, M. S. Brandt, T. Graf, O. Ambacher, J. A. Majewski, and M. Stutzmann, g values of effective mass donors in $Al_xGa_{1-x}N$ alloys, Phys. Rev. B 63, 165204 (2010).
8. S. L. Chuang and C. S. Chang, kp method for strained wurtzite semiconductors, Phys. Rev. B 54, 2491 (1996).
9. J. M. Luttinger and W. Kohn, Motion of Electrons and Holes in Perturbed Periodic Fields, Phys. Rev. 97, 869 (1955).
10. J. M. Luttinger, Quantum Theory of Cyclotron Resonance in Semiconductors: General Theory, Phys. Rev., 102, 1030 (1956).